[CANCER RESEARCH 64, 5943–5947, September 1, 2004]

Advances in Brief

XBP1 Is Essential for Survival under Hypoxic Conditions and Is Required for Tumor Growth

Lorenzo Romero-Ramirez,[1] Hongbin Cao,[1] Daniel Nelson,[1] Ester Hammond,[1] Ann-Hwee Lee,[2] Hiderou Yoshida,[4] Kazutoshi Mori,[4] Laurie H. Glimcher,[2,3] Nicholas C. Denko,[1] Amato J. Giaccia,[1] Quynh-Thu Le,[1] Albert C. Koong[1]

[1]Department of Radiation Oncology, Stanford University, Stanford, California; [2]Department of Immunology and Infectious Diseases, Harvard School of Public Health, Boston, Massachusetts; [3]Department of Medicine, Harvard Medical School, Boston, Massachusetts; and [4]Department of Biophysics, Graduate School of Science, Kyoto University, Kyoto, Japan

Abstract

Hypoxia within solid tumors is a major determinant of outcome after anticancer therapy. Analysis of gene expression changes during hypoxia indicated that unfolded protein response genes were one of the most robustly induced groups of genes. In this study, we investigated the hypoxic regulation of X-box binding protein (XBP1), a major transcriptional regulator of the unfolded protein response. Hypoxia induced XBP1 at the transcriptional level and activated splicing of its mRNA, resulting in increased levels of activated XBP1 protein. After exposure to hypoxia, apoptosis increased and clonogenic survival decreased in XBP1-deficient cells. Loss of XBP1 severely inhibited tumor growth due to a reduced capacity for these transplanted tumor cells to survive in a hypoxic microenvironment. Taken together, these studies directly implicate XBP1 as an essential survival factor for hypoxic stress and tumor growth.

Introduction

Hypoxia is a physiologically important endoplasmic reticulum (ER) stress common to all solid tumors. Numerous clinical studies have demonstrated that tumor hypoxia predicts for decreased local control, increased distant metastases, and decreased overall survival in a variety of human tumors (1). Hypoxia selects for tumors with an increased malignant phenotype (2) and increases the metastatic potential of tumor cells (3). Understanding the role of hypoxia in tumorigenesis and its influence on anticancer therapy is crucial to improving current cancer treatments (4).

The ER is an extensive intracellular membrane network that extends throughout the cytoplasm and functions primarily to process newly synthesized secretory and transmembrane proteins. Accumulation of unfolded proteins in this compartment causes ER stress and prolonged ER stress ultimately results in cell death. The cellular response to ER stress consists of at least two coordinated pathways: (1) rapid translational arrest mediated by pancreatic ER kinase or PKR-like ER kinase (PERK); and (2) transcriptional activation of unfolded protein response target genes (5, 6). In addition to cancer (7), the unfolded protein response has therapeutic implications in diseases such as diabetes, atherosclerosis, viral infection, conformational diseases, and cerebrovascular disease (8).

Koumenis *et al.* (9) previously demonstrated that translational control of protein synthesis during hypoxia occurs through the activation of PERK. These investigators showed that PERK$^{-/-}$ mouse embryonic fibroblasts where unable to phosphorylate eIF2α and had decreased survival during hypoxia when compared with wild-type mouse embryonic fibroblasts. They concluded that PERK plays an important role in hypoxia-induced translation attenuation, additionally supporting a role for hypoxia as an inducer of ER stress (9). When the PERK-dependent translational attenuation pathway is activated, activating transcription factor-4 (ATF-4) mRNA is selectively translated, leading to an induction of ATF-4 downstream target genes (10). Moreover, ATF-4 protein has also been shown to be stabilized in a hypoxia-induced factor 1(HIF-1)-independent manner during anoxia (11).

Previous studies have demonstrated that during ER stress, an ER transmembrane endoribonuclease (IRE1) oligomerizes, autophosphorylates, and uses its endoribonuclease activity to excise a 26 nucleotide intron from unspliced X-box binding protein 1 (XBP1) mRNA (12). These events result in the production of a potent XBP1 transcription factor that regulates a distinct set of unfolded protein response target genes (13).

In this study, we analyzed global changes in gene expression during hypoxia and found that unfolded protein response-related genes, including genes specifically regulated by XBP1, were most robustly induced during severe hypoxia/anoxia. Because of its role as a major transcriptional activator of these genes and its overexpression in some tumor types (14), we investigated the effect of hypoxia on XBP1 regulation. Most importantly, we present evidence that loss of XBP1 increases the sensitivity of transformed cells to killing by hypoxia and severely impedes tumor growth. Because loss of XBP1 had little effect on the secretion of proangiogenic factors such as vascular endothelial growth factor (VEGF) and basic fibroblast growth factor, the mechanism of impaired tumor growth in XBP1-deficient cells is likely not dependent upon angiogenesis and is a direct consequence of impaired survival of XBP1-deficient cells under hypoxic conditions. These studies support the concept of targeting XBP1 as a therapeutic strategy to eliminate hypoxic cells and inhibit tumor growth.

Materials and Methods

Cell Culture and Hypoxia Treatments. HIF-1α wild-type and knockout mouse embryonic fibroblasts, XBP1 wild-type and knockout mouse embryonic fibroblasts, and HT1080 cells (human fibrosarcoma cell line) were maintained in DMEM supplemented with 10% fetal bovine serum at 37°C in a 5% CO_2 incubator. For all hypoxia experiments, cells were treated at 70 to 80% confluency and maintained in an anaerobic chamber (Sheldon Corp., Cornelius, OR) with pO_2 levels $< 0.02\%$.

Gene Expression Studies. Mouse genome MGU74Av2 GeneChip arrays (Affymetrix, Santa Clara, CA) were used for mRNA expression profiling. The preparation of samples and hybridization were carried out as described by Affymetrix. In brief, total RNA from *ras*/c-myc–transformed mouse embryonic fibroblasts exposed to 8 hours of hypoxia were prepared using Trizol

Received 5/7/04; revised 7/7/04; accepted 7/20/04.

Grant support: Eli Lilly-Damon Runyon Clinical Investigator Award (A. Koong), Basque Country Government Grant BFI01.424 (L. Romero-Ramirez), National Cancer Institute Grant CA67166 (Q-T. Le, N. Denko, A. Giaccia), and NIH Grants AI32412 (L. Glimcher) and 1PO150CA100707 (L. Glimcher, A-H. Lee).

The costs of publication of this article were defrayed in part by the payment of page charges. This article must therefore be hereby marked *advertisement* in accordance with 18 U.S.C. Section 1734 solely to indicate this fact.

Requests for reprints: Albert Koong, Stanford University, Department of Radiation Oncology, 269 Campus Drive, CCSR-1245C, Stanford, CA 94305-5152. Phone: (650) 723-7371; Fax: (650) 723-7382; E-mail: akoong@stanford.edu.

(Invitrogen, Carlsbad, CA). Biotinylated RNA was then synthesized using the BioArray RNA transcript labeling kit (Enzo, Farmingdale, NY). Arrays were hybridized with biotinylated *in vitro* transcription products for 16 hours at 45°C according to the manufacturer's instructions. The Fluidic Station 400 (Affymetrix) was used for washing, and a three-step staining protocol was used to enhance detection of the hybridized biotinylated RNA. Arrays were scanned by the Affymetrix fluorescence reader (Hewlett Packard). The raw image DAT data files were initially processed using Affymetrix GeneChip software (version 5) to create CEL files. Higher level analysis of microarray CEL files was performed using dChip v1.3 (15) Thorough statistical analysis was carried out using the dChip software (15, 16).

XBP1 Small Interfering RNA (siRNA) Studies. XBP1 wild-type mouse embryonic fibroblasts were infected with a retroviral vector (SFGΔ U3neo), containing an XBP1-specific siRNA sequence as described previously (17). Control cells were infected with the SFGΔ U3neo empty vector alone. After infection, all cells were selected with 0.5 mg/mL G418 for 10 days. Suppression of XBP1 expression was confirmed by standard Northern and Western blotting techniques as described below.

RNA Isolation and Northern Blotting. Total RNA was isolated with Trizol according to the manufacturer's protocol (Invitrogen). Total RNA was denatured with glyoxal (Fisher, Pittsburgh, PA), size fractioned on 1% agarose/sodium phosphate gels, transferred to nylon membranes (Schleicher & Schuell, Keene, NH) and UV cross-linked. Human GRP78, GRP94, XBP1, and VEGF cDNA probes were obtained from American Type Culture Collection (Manassas, VA). Mouse ERDJ4, Herp, $p58^{IPK}$, XBP1, and Glut-1 probes were cloned using specific PCR primers. All probes were verified by sequencing. Probes were labeled with ^{32}P by random priming (Rediprime; Amersham-Pharmacia, Little Chalfont, United Kingdom). Membranes were hybridized in Churches buffer (2% BSA, 7% SDS, 1 mmol/L EDTA in 0.5 mol/L Tris-HCl (pH 7)] at 65°C overnight. The membranes were washed to a stringency of 2× SSC/0.2% SDS at 65°C, exposed to PhosphoImager film (Amersham-Pharmacia) overnight, and visualized on a Storm 860 PhosphoImager (Molecular Dynamics, Amersham). Ribosomal 28S RNA was used as a loading control.

Western Blotting. Cell extracts were prepared in 9 mol/L urea, 75 mmol/L Tris-HCl (pH 7.5), and 0.15 mol/L β-mercaptoethanol (Sigma, St. Louis, MO), sonicated briefly, boiled at 95°C for 5 minutes, and loaded onto SDS-PAGE gels. After electrophoresis, the proteins were transferred onto a nitrocellulose membrane (Bio-Rad, Hercules, CA) and blocked in 5% nonfat milk with 0.1% Tween 20 in Tris-buffered saline for 30 minutes at room temperature. XBP1 protein was detected using an antibody specific to the spliced and unspliced forms as described previously (12).

Survival and Apoptosis Assay. Cells previously treated in the hypoxia chamber were plated in tissue culture dishes in triplicate at different densities ranging from 300 to 500,000 cells per dish. Plating efficiency was determined by harvesting untreated cells. After 10 to 14 days, the cells were fixed and stained with a solution of 0.25% crystal violet in ethanol. Surviving fraction was determined by counting the number of colonies with >50 cells. Surviving fraction was normalized by the plating efficiency. The results represent the mean of three independent experiments with the error bars representing ±1SD.

For the apoptosis experiments, 10^6 cells were plated in 10-cm tissue culture dishes and placed into the hypoxia chamber for 24 and 48 hours. Untreated cells (normoxic) cells were plated at the same density and maintained in a 37°C incubator. After the treatment, cells were trypsinized and stained with terminal deoxynucleotidyl transferase-mediated nick end labeling (TUNEL) antibody according to the manufacturer's protocol (Roche Diagnostics, Indianapolis, IN). Apoptotic cells were visualized and quantitated by fluorescence activated cell sorting (Becton Dickinson, San Jose, CA). Results represent the mean of four independent experiments with the errors bars representing ±1 SD.

Tumor Growth. Cells (2×10^6) and (5×10^6) were implanted s.c. into the flanks of SCID mice. Each mouse was implanted with spontaneously transformed mouse embryonic fibroblasts that were either XBP1 wild-type or XBP1 knockout. In separate experiments, SCID mice were also implanted with XBP1 wild-type mouse embryonic fibroblasts and siRNA XBP1 mouse embryonic fibroblasts (ix-XBP1). Tumor volume was calculated according to the following formula: $V\ (mm^3) = (L \times l \times \text{hours} \times \pi)/6$, where L is the length, l is the width, and h the height of the tumor, respectively. The error bars represent ±1 SD of the mean volume. For the *in vitro* cell proliferation assays, XBP1 wild-type and -deficient cells were plated in equal cell numbers and counted during logarithmic growth phase.

Secretion Assays. Cells (4×10^5) were seeded in 6-cm dishes and incubated overnight. Fresh media were added, and cells were exposed to 6 and 24 hours of normoxia or hypoxia. VEGF was measured by ELISA according to the manufacturer's protocol (R&D Systems, Indianapolis, IN). Basic fibroblast growth factor was detected using a mouse monoclonal antibody (Transduction Laboratories, Lexington, KY) at 1:1000 dilution. All data are reported as a fold induction relative to normoxic controls. These experiments represent the pooled results of two independent experiments with the error bars representing 1 SD of the mean.

A

Gene	Accession	Fold Change
DNA-damage inducible transcript 3/Chop	X67083	61
HERP	AI846938	24
Activating transcription factor 3	U19118	23
ERO1-like (S. cerevisiae)	AA798624	22
$P58^{IPK}$	U28423	14
ERDJ4	AI835630	10
Solute carrier family 2, member 1 (GLUT-1)	M22998	9
ARMET	AW122364	8
HEDJ	AW122551	5
Coproporphyrinogen oxidase	D16333	5
GRP78 (Bip)	AJ002387	5
X-box binding protein 1	AW123880	5
Asparagine synthetase	U38940	4
Glucosamine-phosphate N-acetyltransferase1	AW123026	4
Activating transcription factor 4	M94087	4
Pentaxin related gene	X83601	3
SEC61, alpha subunit (S. cerevisiae)	AI838624	2.5
GRP94	J03297	2

B

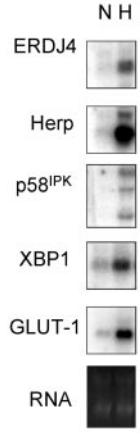

Fig. 1. *A*, rank list of hypoxia-regulated UPR genes that were induced ≥2-fold using the mouse 12,000 gene MGU74Av2 GeneChip. These experiments were repeated in six independent experiments to minimize experimental variability. *B*, Northern blot analysis to confirm the induction of unfolded protein response genes by hypoxia (8 hours).

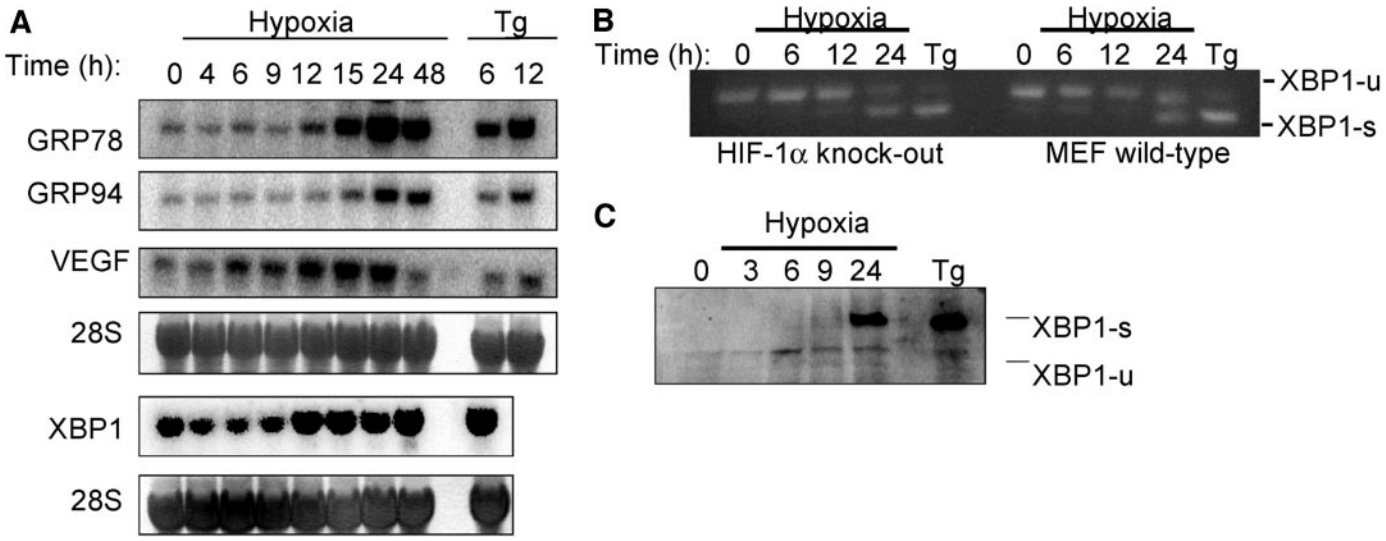

Fig. 2. *A*, GRP78, GRP94, XBP1, and VEGF mRNA expression increased during hypoxia in HT1080 cells. Treatment with 300 nmol/L thapsigargin (Tg), an inhibitor of the Ca-ATPase, was included as a positive control for UPR induction. *B*, HIF-1 wild-type and -knockout mouse embryonic fibroblasts (MEFs) demonstrated similar splicing of XBP1 mRNA during hypoxia. *C*, Spliced XBP1 protein was induced during hypoxia in HT1080 cells.

Results and Discussion

Ras and c-myc transformed mouse embryonic fibroblasts were exposed to severe hypoxia/anoxia (0.02% O_2) for a period of 8 hours before total RNA was isolated from both normoxic and hypoxic samples for microarray analysis. This experiment was repeated six times to minimize experimentally introduced variations. Among the 12,000 genes present on the MGU74Av2 GeneChip, 285 were found to be induced by at least 2-fold (2.4%). Of the top 30 most robustly induced genes under severe hypoxia/anoxia, 25% were involved in the unfolded protein response. Fig. 1*A* is a compilation of known unfolded protein response genes that were induced ≥2-fold during hypoxia. We confirmed by Northern blotting that many of these unfolded protein response genes were transcriptionally induced under hypoxia (Fig. 1*B*).

Next, we investigated the kinetics of unfolded protein response induction under severe hypoxia/anoxia. Overall, the time course for transcriptional activation of unfolded protein response genes was slower than for HIF-1–regulated genes (Fig. 2*A*). The induction of VEGF by severe hypoxia/anoxia was rapid compared with the unfolded protein response genes (GRP78, GRP94, and XBP1), and the expression of unfolded protein response genes remained elevated during prolonged periods of severe hypoxia/anoxia (48 hours) while VEGF mRNA decreased (Fig. 2*A*). This decrease in VEGF mRNA corresponded with a similar decrease in HIF-1α protein (data not shown). Furthermore, the induction of unfolded protein response genes was not evident under less severe hypoxic (2% O_2) conditions (data not shown).

The generation of the active spliced form of XBP1 was assayed by PCR amplification with primers specific to the spliced and unspliced forms of XBP1 in HIF-1 wild-type and HIF-deficient mouse embryonic fibroblasts. The splicing occurred with equal efficiency during hypoxia in both cell lines, indicating that XBP1 activation occurs in a HIF-1–independent manner (Fig. 2*B*). Spliced XBP1 mRNA was efficiently translated into the proteins of XBP1 during severe hypoxia/anoxia as evidenced by immunoblotting with XBP1-specific antibody (Fig. 2*C*).

To determine the role for XBP1 in cell survival during these conditions, we compared the amount of apoptosis in cell cultures of XBP1 wild-type and XBP1-deficient mouse embryonic fibroblasts by TUNEL staining (Fig. 3*A*). After 48 hours of hypoxia, 62.7 ± 11.8% of the XBP1-knockout cells stained positive for TUNEL staining, whereas only 38.6 ± 9.3% of the wild-type cells stained positive for TUNEL. Under normoxic conditions, 4.5 ± 3.7% of the XBP1-deficient cells and 7.8 ± 4.0% of the wild-type cells stained positive for TUNEL. These data represent the mean of four independent experiments ±1 SD. These results indicate that XBP1-deficient cells are more sensitive to hypoxia-induced apoptosis than XBP1 wild-type cells and are consistent with published data showing increased apoptosis during ER stress in myeloma cells, expressing either a dominant negative or a siRNA vector to inhibit XBP1 expression (17).

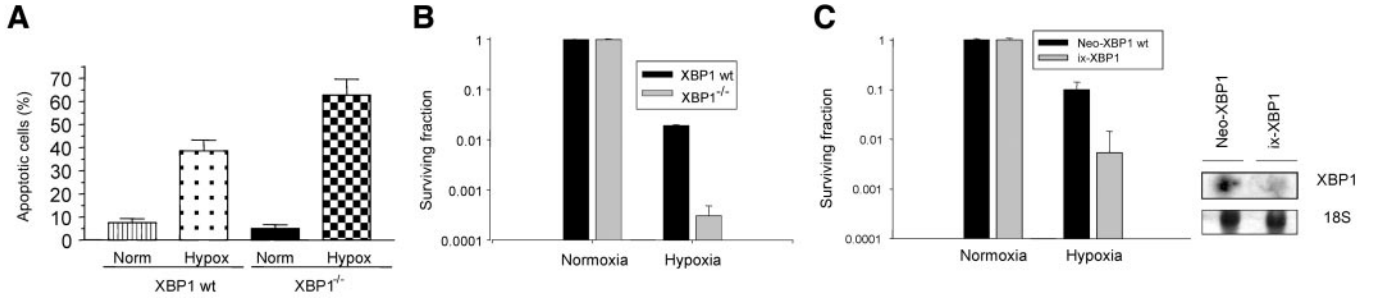

Fig. 3. Comparison of apoptosis after 48 hours of hypoxia between (*A*) XBP1 wild-type and -knockout MEFs. *B*, comparison of clonogenic survival in XBP1 wild-type and -knockout MEFs (*left panel*). Comparison of clonogenic survival in control MEFs (neo-XBP1) and siRNA XBP1-knockdown cells (ix-XBP1; *right panel*). *Far right panel* was included to demonstrate that XBP1 expression was reduced in cells stably transfected with XBP1 siRNA construct.

A

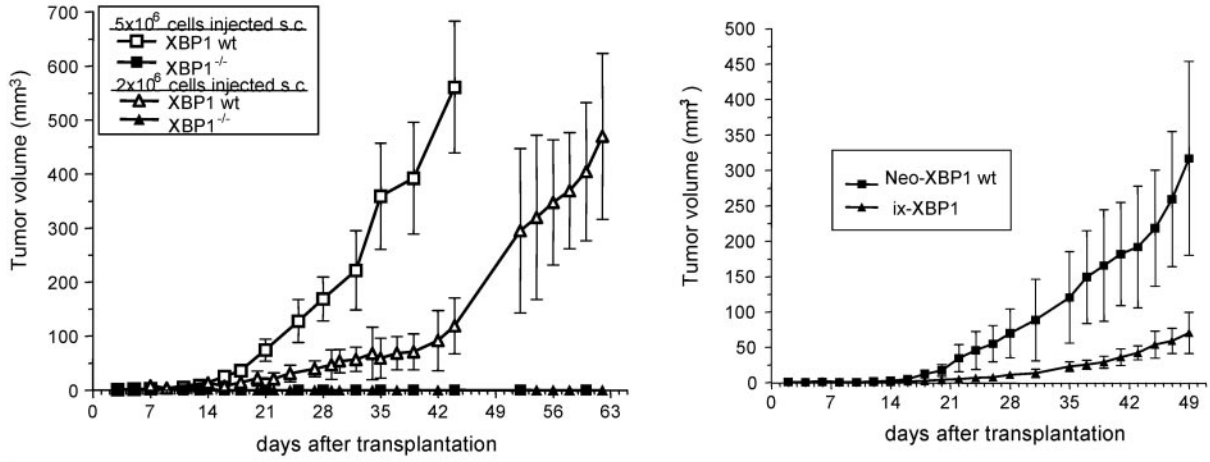

B

Summary of tumor growth delay experiments

Cells transplanted	Number of cells transplanted	Tumor volume (mm^3)	Tumor weight (g)	Tumor formed / Mice transplanted	Weeks after transplantation
XBP1-wt cells	$2x10^6$	469.6±54.3	1.34±0.26	8/8	9
XBP1 (-/-) cells	$2x10^6$	0	0	0/8	9
XBP1-wt cells	$5x10^6$	560.8±121.7	2.05±0.78	4/4	6
XBP1 (-/-) cells	$5x10^6$	0	0	0/4	9
Neo-XBP1-wt cells	$2x10^6$	316.8±137.1	1.27±0.42	7/7	7
ix-XBP1 cells	$2x10^6$	70.4±29.0	0.39±0.13	7/7	7

C

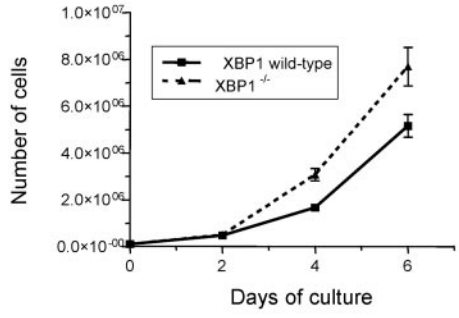

D

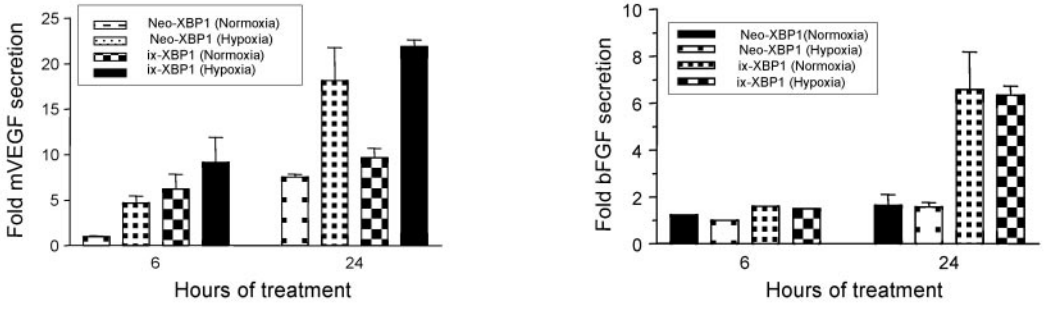

Fig. 4. XBP1 is essential for tumor growth. *A*, Each SCID mouse was implanted subcutaneously with two tumors consisting of 2×10^6 XBP1 wild-type cells in one flank and either 2×10^6 knockout cells or 2×10^6 ix-XBP1 cells in the contralateral flank. In a separate experiment, 5×10^6 XBP1 wild-type or -knockout cells were implanted into separate mice. The XBP1-knockout cells were not able to grow as tumors, and the XBP1-knockdown cells demonstrated a 4-fold tumor growth delay. *B*, summary of the tumor volume and weights at the completion of the tumor growth delay experiments. *C*, comparison of *in vitro* growth rates between XBP1 wild-type and -deficient cells. *D*, comparison of secretion of proangiogenic factors VEGF and basic fibroblast growth factor in the XBP1 control and -knockdown cells. *Error bars* represent 1 SD of the mean from two independent experiments.

Clonogenic survival was reduced 65-fold in the XBP1-knockout mouse embryonic fibroblasts compared with wild-type mouse embryonic fibroblasts during severe hypoxia/anoxia. (Fig. 3*B*). To further support the role of XBP1 in mediating survival during hypoxia, we also analyzed clonogenic survival in XBP1 wild-type mouse embryonic fibroblasts stably transfected with a siRNA vector to inhibit XBP1 expression. These XBP1 knockdown cells (ix-XBP1) exhibited reduced expression of XBP1 (<10% compared with control cells) and showed a similar decrease (19-fold) in clonogenic survival during severe hypoxia/anoxia as compared with the knockout cells (Fig. 3*B*). Interestingly, although inhibition of XBP1 by siRNA reduced clonogenic survival under severe hypoxia/anoxic conditions, the small amount of XBP1 remaining affords significant protection to these cells. Therefore, complete loss of XBP1 has far more profound effects on survival than inhibition of XBP1.

We implanted XBP1 wild-type, XBP1-deficient, or XBP1 siRNA-transfected cells (either 2×10^6 or 5×10^6 cells) into the flanks of SCID mice to determine whether the differences that we found in clonogenic survival during hypoxic conditions *in vitro* translated into impaired tumor growth in XBP1-deficient cells. In each mouse, we implanted XBP1 wild-type cells in one flank and either XBP1-knockout cells or XBP1 siRNA-transfected cells (ix-XBP1) in the contralateral flank. We performed serial tumor measurements up to 63 days (XBP1-knockout cells; Fig. 4*A*, left panel) and 49 days (ix-XBP1, Fig. 4*A*, right panel) after implantation. The XBP1-knockout cells were unable to grow as tumors, whereas the ix-XBP1 cells showed a 4-fold delay in tumor growth rate. We attribute the slower tumor growth rate in the ix-XBP1 cells to incomplete suppression of XBP1 by the siRNA vector. The tumor weights at the time the mice were sacrificed are summarized in Fig. 4*B*. Mice bearing XBP1 wild-type tumors were also received injections of EF5, a nitroimidazole that forms intracellular adducts under hypoxic conditions (18). Immunohistochemical staining of these tumor sections with EF5- and XBP1-specific antibodies showed excellent colocalization of XBP1 expression with areas of hypoxia (data not shown).

To confirm that the differences in tumor growth rates could not simply be attributed to a difference in cell proliferative capacity, we compared the *in vitro* growth rates of XBP1 wild-type and XBP1-deficient cells. The growth rates between these cell types were similar. In fact, the XBP1-deficient cells grew slightly faster than the wild-type cells (Fig. 4*C*).

Because tumor growth requires cells to survive long enough to form a multicellular mass and secrete proangiogenic growth factors, we investigated whether the differences in tumor growth between XBP1 wild-type and -deficient cells were due to a defect in the secretion of proangiogenic factors such as VEGF or basic fibroblast growth factor. We found that this was not the case as XBP1-deficient cells actually secreted a higher basal level of fibroblast growth factor, whereas VEGF secretion was similar at baseline and in response to severe hypoxia/anoxia in XBP1 wild-type and -deficient cells (Fig. 4*D*).

Taken together, these studies strongly support a role for XBP1 in mediating survival during hypoxia and in regulating tumor growth. Before the establishment of an adequate blood supply, tumor cells must be able to survive in a microenvironment that is deficient in oxygen, ATP, and other essential nutrients. Under these conditions, the response to ER stress is critical for cell survival. The unfolded protein response pathway functions independently of HIF-1α and directly links XBP1 with tumorigenesis, leading us to conclude that hypoxic regulation of the unfolded protein response is fundamentally important in the development of tumors. Although the exact mechanism for this observation remains to be elucidated, other components of the unfolded protein response pathway are also likely involved. Furthermore, because XBP1-deficient cells were unable to grow as tumors, it is unclear whether XBP1 is essential for establishment of a tumor, regulation of its subsequent growth, or both processes. Future experiments are directed at defining this mechanism.

Acknowledgments

We thank Dr. Costas Koumenis for insightful discussions and Erin Christofferson for administrative assistance on this project.

References

1. Vaupel P, Kelleher D, Hockel M. Oxygen status of malignant tumors: pathogenesis of hypoxia and significance for tumor therapy. Semin Oncol 2001;28(2 Suppl 8):29–35.
2. Graeber T, Osmanian C, Jacks T, Housman D, Koch C, Lowe S. Hypoxia-mediated selection of cells with diminished apoptotic potential in solid tumours. Nature (Lond.) 1996;379:88–91.
3. Subarsky P, Hill R. The hypoxic tumour microenvironment and metastatic progression. Clin Exp Metastasis 2003;20:237–50.
4. Brown J. Tumor microenvironment and the response to anticancer therapy. Cancer Biol Ther 2002;1:453–8.
5. Ron D. Translational control in the ER stress response. J Clin Investig 2002;110:1383–8.
6. Harding H, Calfon M, Urano F, Novoa I, Ron D. Transcriptional and translational control in the mammalian unfolded protein response. Annu Rev Cell Dev Biol 2002;18:575–99.
7. Lee A. The glucose-regulated proteins: stress induction and clinical applications. Trends Biochem Sci 2001;26:504–10.
8. Kaufman R. Orchestrating the unfolded protein response in health and disease. J Clin Investig 2002;110:1389–98.
9. Koumenis C, Naczki C, Koritzinsky M, et al. Regulation of protein synthesis by hypoxia via activation of the ER kinase PERK and phosphorylation of the translation initiation factor eIF2alpha. Mol Cell Biol 2002;22:7405–16.
10. Harding H, Novoa I, Zhang Y, et al. Regulated translation initiation controls stress-induced gene expression in mammalian cells. Mol Cell 2000;6:1099–108.
11. Ameri K, Lewis C, Raida M, Sowter H, Hai T, Harris A. Anoxic induction of ATF-4 through HIF-1–independent pathways of protein stabilization in human cancer cells. Blood 2004;103:1876–82.
12. Yoshida H, Matsui T, Yamamoto A, Okada T, Mori K. XBP1 mRNA is induced by ATF6 and spliced by IRE1 in response to ER stress to produce a highly active transcription factor. Cell 2001;107:881–91.
13. Lee A, Iwakoshi N, Glimcher L. XBP-1 regulates a subset of ER resident chaperone genes in the unfolded protein response. Mol Cell Biol 2003;23:7448–59.
14. Fujimoto T, Onda M, Nagai H, Nagahata T, Ogawa K, Emi M. Up-regulation and overexpression of human X-box binding protein 1 (hXBP-1) gene in primary breast cancers. Breast Cancer 2003;10:301–6.
15. Li C, Wong W. Model-based analysis of oligonucleotide arrays: expression, index computation and outlier detection. Proc Natl Acad Sci USA 2001;98:31–6.
16. Li C, Hung Wong W. Model-based analysis of oligonucleotide arrays: model validation, design issues and standard error application. Genome Biol 2001;2:1–11.
17. Lee A, Iwakoshi N, Anderson K, Glimcher L. Proteosome inhibitors disrupt the unfolded protein response in myeloma cells. Proc Natl Acad Sci 2003;100:9946–51.
18. Koch C. Measurement of absolute oxygen levels in cells and tissues using oxygen sensors and the 2-nitroimidazole EF5. In: Packer A, editor. Antioxidants and redox signaling. San Diego, CA: Academic Press; 2001. p. 3–31.